MINERALOGICAL MAGAZINE, JUNE 1980, VOL. 43, PP. 701–14

Anatexis and high-grade metamorphism in the Champira Dome, Malawi: petrological and Rb–Sr studies

H. W. HASLAM, M. S. BREWER,* A. E. DAVIS, AND D. P. F. DARBYSHIRE

Institute of Geological Sciences, 64–78 Gray's Inn Road, London WC1X 8NG

SUMMARY. Banded gneisses and migmatites in the Champira Dome contain assemblages of the biotite-cordierite-almandine subfacies of the granulite facies. The banded gneisses represent a sequence of arkosic sediments metamorphosed to sillimanite-cordierite gneisses. The migmatites were derived from more argillaceous and potassic sediments, with lower oxidation ratios and lower Ba/Rb ratios. They consist of a quartzo-feldspathic leucosome, representing anatectic melt, with schlieren of the refractory minerals sillimanite, garnet, biotite, and oxide minerals. Cordierite developed from garnet and biotite, except in rocks of high FeO/(FeO + MgO) ratio. Both rock types contain assemblages of magnetite + hercynite + corundum + ilmenite + hematite, formed by unmixing of high-temperature solid solutions. Rb-Sr studies of the banded gneisses gave an age of 2327 ± 25 Ma, which is interpreted as the date of metamorphism, and an initial $^{87}Sr/^{86}Sr$ ratio of 0.7064 ± 0.0003. The migmatite samples plot close to this 2327 Ma regression line, but the strontium isotopes were considerably disturbed, though not homogenized on the scale of sampling, 962 ± 34 Ma ago. It is considered that the anatexis in the migmatites was contemporaneous with the metamorphism of the banded gneisses and that the 962 ± 34 Ma event may be correlated with recrystallization of the migmatites accompanying the growth of cordierite.

THE Champira Dome (fig. 1A) consists largely of banded sillimanite-cordierite-garnet gneisses. It was emplaced as a tectonic wedge between ENE-trending boundary faults and appears to have a different structural and metamorphic history to that of the surrounding rocks (Peters, 1975). The purpose of this paper is to elucidate as far as possible the origins and metamorphic history of the rocks of the dome. Two suites of specimens were examined. Specimens MB 52 and 54–59 are banded gneisses. To the north-east of these (fig. 1B) is an area of migmatite (MB 53 and 60–65). Both suites contain mineral assemblages characteristic of the biotite-cordierite-almandine subfacies of the granulite facies (as defined by de Waard, 1965).

The mineral compositions given in this paper were obtained by electron microprobe, using the techniques and standards described by Bowles (1975) and the correction programme of Mason *et al.* (1969). For oxide minerals, each composition given is the mean of two analyses obtained from a single crystal cluster. For silicate minerals, each composition is the mean of four analyses—two

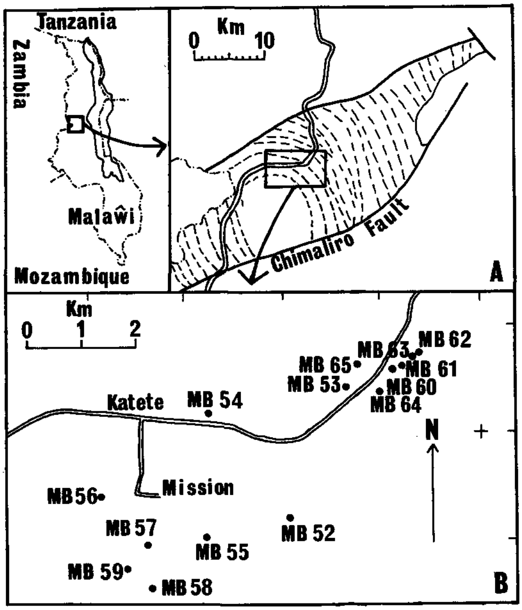

FIG. 1. A. Outline of the Champira Dome (after Peters, 1975), showing the structural trends in the banded garnet-sillimanite-cordierite gneisses of the dome. B. Sample localities; intervals of 1 minute are marked on the northern and eastern edges of the map, and the point with coordinates 12° 20′ S 33° 40′ E is indicated near the eastern edge of the map.

---

* Present address: Bermuda College, Department of Academic Studies, Prospect, Devonshire 4-04, Bermuda.

from each of two small areas of a single rock section, representing both core and margin. No compositional zoning was noted. Partial analyses of feldspars were obtained with the beam scanning an area of about 17 μm by 24 μm in order to reduce the effects of unmixing and other compositional variation.

Migmatites

The migmatite specimens (MB 53 and 60–65, Tables I and II) are composed of coarse-grained quartzo-feldspathic leucosomes containing scattered crystals of garnet and patches and schlieren of dark minerals. Sample 61L (Table II) is a 400 g portion of MB 61 which was essentially free of mafic minerals. Rock types transitional between the banded gneisses and these migmatites are exposed near MB 64 and near MB 65.

The leucosomes in the migmatite specimens consist of orthoclase microperthite and quartz, with subordinate sodic plagioclase. The quartz shows the bluish coloration characteristic of the granulite facies. The other minerals, which occur in part as discrete crystals but mainly clustered together in schlieren, are biotite, sillimanite, garnet, cordierite, magnetite, hercynite (green to opaque in transmitted light), ilmenite, and corundum. The cordierite in some sections is altered to a yellow isotropic material. Mineral abundances are given in Table I, based on sections of one to six hand specimens of each sample (only one or two specimens for the opaque minerals). In most sections one or more of the phases are absent but a few slides show them all. Monazite, zircon, and apatite are sporadic accessory minerals, and a few specimens contain a little secondary white mica. The magnetite in MB 61 contains hematite lamellae.

A small basic xenolith enclosed in migmatite close to MB 64 consists largely of labradorite and pleochroic hypersthene, with subordinate biotite, quartz, hornblende, clinopyroxene, apatite, and iron oxides. The presence of orthopyroxene and the absence of cordierite can be attributed to a higher $(FeO+MgO)/Al_2O_3$ ratio in the rock.

Oxide minerals. Hercynite, magnetite, and ilmenite in MB 62 have the approximate compositions $(Fe^{2+}{}_{6.3}\,Mn_{0.1}\,Mg_{1.6})\,(Al_{15.0}\,Cr_{0.1}\,Fe^{3+}{}_{0.9})\,O_{32}$, $Fe^{2+}{}_{8.0}(Al_{0.1}Cr_{0.1}V_{0.2}Fe^{3+}{}_{15.6})O_{32}$, and $(Fe^{2+}{}_{1.85}Mn_{0.06})Ti_{1.91}Fe^{3+}{}_{0.15}V_{0.02}Al_{0.01}O_6$. Coexisting magnetite and ilmenite compositions (Mt:Usp = 99.5:0.5; Hem:Ilm = 3.8:96.2) indicate an equilibration temperature well below 500 °C and f_{O_2} less than 10^{-25} bars (see Buddington and Lindsley, 1964, fig. 5).

The magnetite and hercynite compositions (95 % Fe_3O_4, 1 % $FeAl_2O_4$; 5 % Fe_3O_4, 73 % $FeAl_2O_4$, 20 % $MgAl_2O_4$) also suggest a temperature well below 500 °C (Turnock and Eugster, 1962, fig. 5), though Turnock and Eugster's results cannot be applied strictly to the present data because of the presence of Mg in the hercynite. The occurrence of magnetite, hercynite, and corundum as polymineralic clusters often showing inclusions and

TABLE I. *Abundance of restite minerals in migmatite samples*

Sample No.	MB 53	MB 60	MB 61	MB 62	MB 63	MB 64	MB 65
No. of sections examined	2	8	2	4	2	3	4
Biotite	÷	+P	+	÷	–	+	+
Sillimanite	÷	+	+	+	+	+	+
Garnet	–	+	+	+P	+	+	+
Cordierite	O	+	–	+P	+	O	+
Magnetite	√	√	√	√P	√	√	√
Hercynite	√	√	√	√P	√	√	√
Ilmenite	O	√	√	√P	O	√	√
Corundum	√	√	√	√	√	√	√

Silicate minerals:	
Major constituent in at least one section	+
Minor or trace constituent but consistently present	÷
Minor or absent	–
Not observed	O
Oxide minerals:	
Present	√
Not identified	O
Electron microprobe analysis	P

exsolution textures suggests that they formed from the cooling of a high temperature Fe_3O_4-$FeAl_2O_4$ solid solution (Turnock and Eugster, 1962, fig. 11). This process accounts for the presence of corundum in rocks containing abundant quartz, and shows that oxygen was introduced into the system as the temperature fell. A few clusters show thin rims of garnet, sillimanite, or possible cordierite, but they generally exsolved without significant reaction with the surrounding silicates. The unmixed oxides are too coarse grained to enable estimation of the composition (and hence the minimum temperature of formation) of the primary solid solution.

Silicate minerals. The stability of cordierite in high-grade pelitic rocks has been discussed by many authors, including Winkler (1976), Holdaway and Lee (1977), and Ashworth and Chinner (1978). The coexistence of almandine and cordierite is dependent upon the molar FeO/(FeO + MgO) ratio of the rock (high values of this ratio favour almandine); temperature (higher temperatures favour almandine); total pressure (higher pressures favour almandine); and P_{H_2O} (at constant P_{tot}) (drier conditions favour almandine). In the migmatite suite, cordierite appears to be absent from MB 64 (FeO/(FeO + MgO) = 0.65); it is present in trace quantities in MB 61 (0.63); and it is generally abundant, with surviving garnet, in MB 60, 62, 63, and 65 (0.53-0.63). MB 53 contains a little garnet but no cordierite; the FeO and MgO contents (Table II) are too low to allow much confidence in the value of 0.5 obtained for the FeO/(FeO + MgO) ratio.

Reaction textures, though partly obscured by over-all recrystallization of the rock, indicate that cordierite grew at the expense of garnet, sillimanite, and biotite. The replacement of biotite plus sillimanite by cordierite releases $KAlSi_3O_8$. The absence of any non-perthitic (i.e. low soda) alkali feldspar adjacent to cordierite in thin section implies that the newly released orthoclase was incorporated into reconstituted soda-bearing alkali feldspar.

In MB 62, garnet of composition $(Fe_{3.82}Mn_{0.46}Mg_{1.30}Ca_{0.15})Al_{4.01}Si_{6.10}O_{24}$ coexists with, and has been partially replaced by, cordierite of composition $(Fe_{0.49}Mn_{0.02}Mg_{1.37})Al_{3.92}Si_{5.11}O_{18}$. Plotting these compositions on fig. 6 of Holdaway and Lee (1977) gives 675 ± 50 °C at 7-8 kb, but dilution of the phases in the assemblage lowers the pressure of the reaction curves. The assemblage almandine + cordierite + alkali feldspar + quartz requires $P_{H_2O} < P_{tot}$, although the presence of biotite requires $P_{H_2O} \geqslant 0.4\ P_{tot}$ (Holdaway and Lee, 1977). The garnet contains about 11 % (grossular + spessartine) and the alkali feldspar contains about 22 % (Ab + An). The effects of these impurities is to lower the temperature of the Bio + Sl + Q = Cd + G + Kfel + V equilibrium further than given by fig. 7B of Holdaway and Lee (1977). This could have the effect of lowering the point where cordierite with X_{Fe}(Fe/(Fe + Mg)) = 0.26 can coexist with garnet, with or without biotite, to just below the granite melting curve at $P_{H_2O} = 0.4\ P_{tot}$, i.e. about 675 °C and 5 kb. This is thus the best estimate obtainable for the conditions of formation of the cordierite.

Analysed cordierite crystals not associated with garnet but occurring in the same section of MB 62 are more iron-rich ($X_{Fe} = 0.33$) than those which are associated with garnet. The reason for this is not clear, but one possible explanation is that the independent grains are of an earlier generation. Alternatively, there may have been some retrograde reaction in the cordierite in contact with garnet.

Biotite in MB 60 (a sample which contains abundant cordierite) has an approximate composition $(K_{1.73}Na_{0.28})Fe_{1.34}Mn_{0.01}Mg_{4.06}Ti_{0.41}Al_{2.66}Si_{5.39}O_{20}(OH)_4$. Comparison of this composition with fig. 3 of Holdaway and Lee (1977) shows that at 675 °C the pressure would have to be in excess of 4.5 kb at $P_{H_2O} = P_{tot}$, and, if the likely effects of the dilution of the phases are taken into account, the pressure is unlikely to be less than 5 kb.

Approximate feldspar compositions in MB 62 ($An_{33}Ab_{66}Or_1$ and $An_1Ab_{21}Or_{78}$), applied to the determinative curves of Stormer (1975), indicate an equilibration temperature of about 650 °C at 5 kb.

Chemistry. The MgO content of the migmatite samples may be taken as a measure of the amount of mafic material present: it shows a positive correlation (fig. 2) with other oxides which occur principally in the mafic minerals (TiO_2, FeO(T), MnO) and a negative correlation with oxides which occur predominantly in the felsic minerals (SiO_2, Na_2O, K_2O); Al_2O_3, which occurs in felsic and mafic minerals, shows little variation with decreasing MgO, but normative corundum, which relates to the mafic material, correlates positively with MgO.

The relative proportions of normative Q, Or, and Ab are given in Table II. Compared with the ternary eutectic in the system Q-Or-Ab (31 % Q, 24 % Or, 45 % Ab at 4 kb P_{H_2O}) (Tuttle and Bowen, 1958, fig. 38) the samples are rich in normative Q and Or and poor in normative Ab. The analyses lie on the Or-rich fringe of the distribution of analysed granitic rocks (Tuttle and Bowen, 1958, fig. 42).

On the Or-Ab-An diagram, the samples with a low mafic content (MB 53, 61, and 65) plot in the low-temperature trough (Kleeman, 1965), but again they are notably rich in Or compared with

TABLE II. *Chemical analyses and CIPW norms of rock samples*

	Migmatites								Banded gneisses						
	MB 53	MB 60	MB 61	MB 61L	MB 62	MB 63	MB 64	MB 65	MB 52	MB 54	MB 55	MB 56	MB 57	MB 58	MB 59
SiO_2	75.7	71.3	75.6	75.0	69.9	69.9	71.8	74.4	78.8	79.1	79.8	69.8	82.6	80.8	67.8
TiO_2	0.1	0.5	0.1	0.0	0.3	0.3	0.5	0.3	0.6	0.2	0.6	0.9	0.5	0.6	1.0
Al_2O_3	14.8	15.4	14.6	14.7	15.8	15.8	15.4	14.1	11.3	12.1	11.4	15.9	10.0	11.0	17.5
Fe_2O_3	0.0	0.7	0.3	0.1	0.6	1.0	0.8	1.1	3.2	0.5	4.0	4.7	2.9	3.0	5.6
FeO	0.4	3.6	0.6	0.1	4.3	4.9	3.6	1.8	1.7	1.4	1.4	3.0	1.1	1.2	2.0
MnO	0.0	0.2	0.0	0.0	0.2	0.3	0.2	0.1	0.1	0.0	0.1	0.2	0.1	0.1	0.1
MgO	0.2	1.2	0.2	0.1	1.5	1.9	1.1	0.9	1.2	0.4	1.2	2.1	0.9	1.0	2.2
CaO	1.0	1.8	1.3	1.1	1.4	1.2	1.4	1.1	1.3	0.6	1.0	1.1	1.0	0.9	0.5
Na_2O	2.5	2.7	2.7	2.7	2.4	1.8	2.2	2.1	2.1	2.2	1.5	1.7	1.7	1.7	1.5
K_2O	6.2	3.5	5.6	6.6	4.1	2.8	4.0	4.8	1.7	5.1	1.6	2.7	1.8	1.7	2.9
LoI	0.4	0.1	0.5	0.4	0.1	0.2	0.1	0.6	0.4	0.2	0.5	0.5	0.5	0.4	0.5
H_2O-	0.2	0.2	0.2	0.2	0.2	0.3	0.2	0.3	0.2	0.2	0.2	0.2	0.2	0.2	0.2
P_2O_5	0.1	0.1	0.1	0.1	0.1	0.0	0.1	0.2	0.1	0.1	0.0	0.0	0.0	0.0	0.0
Total	101.6	101.3	101.8	101.1	100.9	100.4	101.4	101.8	102.7	102.1	103.3	102.8	103.3	102.6	101.8
$\frac{FeO}{FeO+MgO}$	0.53	0.63	0.63	0.4	0.62	0.59	0.65	0.53	0.44	0.66	0.40	0.44	0.41	0.40	0.34
O.R.	0.00	0.15	0.30	0.35	0.11	0.16	0.16	0.35	0.63	0.23	0.71	0.58	0.71	0.69	0.71
Norms															
Q	34.9	34.5	35.5	32.0	32.1	39.9	37.0	39.8	55.7	44.4	61.0	44.5	62.5	61.4	43.5
Or	36.3	20.8	33.1	38.9	24.0	16.3	23.8	28.7	10.3	30.2	9.7	15.7	10.5	9.9	17.3
Ab	21.5	22.5	22.6	22.8	20.1	15.1	18.3	17.5	17.7	18.5	12.8	14.0	14.5	14.3	12.9
An	4.5	8.5	5.6	4.5	6.7	5.7	6.4	4.0	6.1	2.2	4.6	5.1	4.8	4.1	2.4
C	2.3	4.1	2.1	1.5	5.1	7.8	5.1	4.0	3.8	2.2	5.4	8.4	3.4	4.9	11.0
Hy	1.1	8.3	1.4	0.3	11.0	12.9	8.1	4.2	2.9	2.8	3.0	5.7	2.1	2.4	5.5
en	0.4	2.9	0.5	0.1	3.7	4.8	2.7	2.3	2.9	0.9	3.0	5.3	2.1	2.4	5.5
fs	0.7	5.4	0.9	0.2	7.3	8.1	5.4	1.9	0.0	1.9	0.0	0.4	0.0	0.0	0.0
Mt	0.0	1.0	0.4	0.1	0.9	1.5	1.1	1.6	3.9	0.7	3.0	6.8	2.2	2.5	4.0
Hm									0.5		1.9		1.4	1.3	2.8
Il	0.1	0.9	0.1		0.6	0.6	0.9	0.6	1.2	0.3	1.2	1.7	0.9	1.1	1.8
Ap	0.2	0.1	0.2	0.3	0.1	0.1	0.1	0.6	0.1	0.2	0.1	0.1	0.1	0.1	0.1
Q	38	44	39	34	42	56	47	46							
Or	39	27	36	42	32	23	30	34							
Ab	23	29	25	24	26	21	23	20							
Trace elements (ppm)															
V	20	48	18	10	46	70	58	33	69	8	74	110	59	65	92
Cr	12	44	17	10	67	92	49	23	76	7	81	115	56	63	91
Ni	6	53	17	3	60	79	47	27	58	10	68	111	47	51	94
Rb	233	95	195	232	134	95	162	173	34	164	40	57	34	27	72
Sr	150	129	145	152	123	90	124	127	141	45	132	145	132	118	146
Zr	58	120	67	1	204	210	144	141	252	185	258	251	263	173	220
Nb	21	24	17	6	18	23	26	19	33	26	23	28	27	21	28
Ba	505	162	325	597	182	116	253	305	152	543	180	331	271	148	294
Ba/Rb	2.2	1.7	1.7	2.6	1.4	1.2	1.6	1.8	4.4	3.3	4.6	5.8	8.0	5.5	4.1

O.R. (Oxidation ratio) = Fe_2O_3/(total Fe as Fe_2O_3)

Grid reference	700375	708378	710378	713381	712380	706374	702379	689351	674370	674347	654355	663346	664338	659341
Weight of sample (kg)														
As collected	30	25	39	14	23	27	26	15	30	23	18	34	32	35
After crushing	26	23	34	13	21	24	23	11	27	18	16	25	28	28

Analyses by A. E. Davis, T. K. Smith, and B. A. R. Tait, using methods described in Brewer *et al.* (1979*a*), Roberts and Davis (1977), French and Adams (1972), and Tait and Coats (1976).

the observed distribution of analyses of granitic rocks (Tuttle and Bowen, 1958, fig. 67; Le Maitre, 1976).

Both the mineralogy and the chemical compositions of the migmatite samples suggest that these rocks were formed by melting of pelitic sediments. The anatectic melting of rocks at 5 kb in the water-saturated system Q-Or-Ab-An was described by Winkler (1976, pp. 285 f.). The samples with a low mafic content (MB 53, 61, and 65) plot in the quartz + liquid + vapour field (idem, fig. 18.8). They contain, respectively, 36, 37, and 44% Q in the Q-Or-Ab-An system, and they all lie quite near the quartz + alkali feldspar + liquid + vapour cotectic surface, which in this area contains about 34% Q. The leucosome from MB 61, with 33% relative Q, plots almost on the cotectic surface, which is consistent with an anatectic origin. Winkler's data show that a water-saturated melt with the composition of MB 61L coexists with quartz, alkali feldspar, and vapour at a temperature of 685 °C at 5 kb or 670 °C at 7 kb. The join of these two points on a P-T plot lies parallel to the granite melting curve. Constraints on the pressure are placed by the presence of sillimanite rather than kyanite (giving a maximum possible pressure of 6.5 kb according to Richardson *et al.* (1969) or 7.5 kb according to Holdaway (1971)) and by the stability of biotite during anatexis (giving a minimum pressure of about 4.5 kb, estimated from the data of Holdaway and Lee (1977)). It therefore seems that, if $P_{H_2O} = P_{tot}$, the minimum conditions of anatexis were around 670–685 °C and 7–5 kb. Were the anatexis not water-saturated, higher temperatures would have obtained, and correspondingly higher P_{tot} would have been required to stabilize biotite.

It is considered that the chemical compositions of the migmatite samples represent the approximate compositions of the parent sediments before anatexis. They appear to have consisted principally of quartz and clays, including a large proportion of potassium-bearing clay minerals. There is no evidence for the introduction of additional material (e.g. K_2O) during anatexis and it is considered improbable that there was any large-scale metasomatism. The widespread distribution and general abundance of small patches of restite mingled with the leucosome leaves no possibility that large quantities of material of another composition could have become separated from the melt. Some differential movement of melt and restite may have been a factor giving rise to the present compositional variation (the restite content decreases, generally, from north-east to south-west), though this could as reasonably be attributed to variations in the composition of the original sediments.

Banded gneisses

The banded gneisses are medium- to coarse-grained rocks with well-developed mineral banding. Samples MB 52 and 55–59 contain quartz, orthoclase microperthite, sillimanite, cordierite, magnetite, and hematite/ilmenite. Minor plagioclase occurs in MB 52 and 56 (which have the highest CaO content) but it is scarce or absent in the other samples. Biotite is absent in MB 56 and 57 but present in small quantities in the other samples. Corundum is present in all the specimens, green spinel in some, and accessory zircon in a few. Yellow isotropic material is a minor replacement product of cordierite.

Sample MB 59 shows evidence of partial melting. Most of the specimen is similar to the other gneisses, but part of it shows a leucosome–restite texture with abundant biotite as well as the common paragenesis.

Specimen MB 54, which differs chemically and mineralogically from the other gneisses, is less well banded. It contains quartz, orthoclase microperthite, hercynite, magnetite, subordinate biotite and garnet, rare oligoclase, corundum, and ilmenite, trace sillimanite, and accessory zircon. Like MB 59 it shows textural evidence of partial melting.

Oxide minerals. The nature of the hematite/ilmenite is related to the oxidation ratio of the rock: MB 56 (O.R. 0.58) contains grains of ilmenite with hematite lamellae, and, rarely, the reverse; MB 52 (0.63) contains hematite with abundant unmixed ilmenite; MB 55 and 57 to 59 (0.69–0.71) contain hematite with minor or very little unmixed ilmenite.

In contrast with the migmatites, corundum occurs with hematite/ilmenite, generally forming broad lamellae, which suggests that this oxide association formed during post-metamorphic cooling by the unmixing of a high temperature Fe_2O_3–$FeTiO_3$–Al_2O_3 solid solution.

Magnetite and ilmenite in MB 56 have approximate compositions ${Fe^{2+}}_{8.0}(Al_{0.1}{Fe^{3+}}_{15.9})O_{32}$ and $({Fe^{2+}}_{1.61}Mn_{0.16}Mg_{0.07})Ti_{1.84}{Fe^{3+}}_{0.30}V_{0.01}Al_{0.01}O_6$. The ilmenite is similar to that in the migmatite but has higher MnO, possibly a consequence of the absence of garnet. As with the migmatite MB 62, the compositions of the magnetite and ilmenite from the banded gneiss MB 56 (Mt:Usp = 99.8; 0.2:Hem:Ilm = 8.6:91.4) indicate an equilibration temperature below 500 °C; f_{O_2}, though less than 10^{-20} bars, was higher than in the migmatite (see Buddington and Lindsley, 1964, fig. 5).

The predominant oxide mineral in MB 54 is hercynite. It is always associated with magnetite (some grains of which show hematite lamellae), sometimes with corundum, and rarely with ilmenite (which also shows hematite lamellae). The associated ore minerals are invariably surrounded by quartz. This texture is a clear indication of replacement, possibly of almandine:

$$3\ Fe_3Al_2Si_3O_{12} + 2[O] = 3\ Fe\ Al_2O_4 + 2\ Fe_3O_4 + 9\ SiO_2$$

Experimental work (Hsu, 1968) showed that in the region of the fayalite + magnetite + quartz buffer this reaction takes place (1) with increasing f_{O_2}, (2) with decreasing T at constant f_{O_2}, (3) with increasing T with buffered f_{O_2}, and (4) with decreasing P_{fluid} at constant T and buffered f_{O_2}, but because garnet also occurs in the rock and shows no signs of reaction, the derivation of the oxides from almandine in MB 54 remains hypothetical.

Silicate minerals. It has been seen that in the migmatites the FeO/(FeO + MgO) ratios span the boundary between garnet and cordierite stability.

In the banded gneisses, MB 52 and 55-59 (0.34-0.44) contain cordierite and no garnet, while in MB 54 (0.66) garnet and hercynite + quartz were apparently stable but there is no cordierite. The texture shows that cordierite formed at the expense of sillimanite, and probably also of biotite. Cordierite in MB 56 has the approximate composition $(Fe_{0.34}Mn_{0.03}Mg_{1.43})Al_{3.93}Si_{5.15}O_{18}$. The absence of samples with FeO/(FeO + MgO) ratios between 0.44 and 0.66 prevents a precise comparison being made with the migmatites, but the cordierite-bearing and garnet-bearing assemblages would be stable over a range of conditions, and within this range lies the set of conditions under which the cordierite-garnet assemblages of the migmatites are stable.

Feldspar compositions in MB 56 (means $An_{35}Ab_{64}Or_1$ and $An_3Ab_{15}Or_{82}$) indicate an equilibration temperature of about 585 °C, with an uncertainty of at least ± 35 °C (see Stormer, 1975).

Chemistry. Chemical analyses of the banded gneisses are given in Table II and plotted, together with the migmatite analyses, in fig. 2. MB 52 and 55-59 plot on near-linear trends. For most elements, the trends are distinctly different from the migmatite trends, an exception being FeO(T). The trends for normative C, unlike those for Al_2O_3, are similar in the two series. The two suites may be distinguished by their oxidation ratios, normative Q, and Ba/Rb ratios (Table II).

Sample MB 54 displays (fig. 2) some features in common with the other gneiss and migmatite samples (TiO_2, FeO(T), MnO and normative C), other features characteristic of the migmatites only (K_2O and oxidation ratio), and others intermediate between the two series (SiO_2, Al_2O_3, Na_2O, and normative Q when plotted against MgO; and the Ba/Rb ratio). The CaO and Sr contents are low and the Rb/Sr ratio is very much higher than in any of the other samples (fig. 3). The collection point of MB 54 (fig. 1) lies between the other two suites and either lateral or vertical facies variation could account for its unique composition.

Winkler (1976, fig. 18-4 and p. 293) showed that for a given pressure in the water-saturated system Q-Or-Ab-An, the beginning of melting takes place at a lower temperature in rocks with more albite-rich plagioclase. If a similar relationship exists when $P_{H_2O} < P_{tot}$, it is noteworthy that the two banded gneisses in which partial melting occurred (MB 54 and 59) are those with the lowest An component, both relative to Ab and absolutely (Table II).

The chemical compositions of the banded gneisses MB 52 and 55-59 suggest that they originated as a sequence of impure quartzose sediments of varying quartz content. The chemical differences show that these sediments do not belong to the same lithotype as the parent sediments of the migmatites, although there is some overlap in major element composition, MB 56 and 63 having very similar contents of all the major elements. The banded gneisses contain consistently higher Ba/Rb ratios than the migmatites. While both Rb and Ba occur predominantly in potassic minerals, the Ba/Rb ratio is generally higher in feldspar than in micas and argillaceous material (Heier and Billings, 1970; Puchelt, 1972). We therefore suggest that, whereas the parent sediments of the migmatites contained a large proportion of potassic clay minerals, those of the banded gneisses contained feldspars as the main potassic minerals. This would also account for the higher K/Rb ratios in the banded gneisses (355-517) compared with the migmatites (207-308) and MB 54 (259). This presence or absence of hydrous phases in the sediments would account for the contrast in the extent of anatexis between the two rock types.

Rb-Sr studies

Sample localities are plotted on fig. 1: grid references and sample weights are given in Table II. Care was taken to collect large (14 kg to 39 kg weight) blocks of the freshest available material to represent true whole-rock systems.

As a measure of the fit of regression lines presented in this paper, a variance ratio (F) statistic is used (see Brewer *et al.*, 1979*a*). Regression results are presented in the following way: the age (A), the regression error (R), and, in parenthesis, the calculated variance ratio (F_c) value. Where appropriate, the 'expanded' error on the age (E) corresponding to the appropriate 5 % value of F is given, viz.: $A \pm R$ Ma (F_c: $\pm E$ Ma). Values for intercepts are given in the same way but omitting repetition of F_c.

The use of expanded errors as a measure of uncertainty is justified even though geological factors that produce the excess scatter probably have a non-gaussian distribution. Expanded errors are those that would have been obtained had the analytical errors been great enough to mask precisely the geological errors at the 95 % confidence level. Clearly such errors refer to a regression line that is indistinguishable from the ideal case.

Analytical data for seven banded gneiss and eight migmatite whole-rock samples (including MB 61L) together with three mineral analyses from sample MB 60 are given in Table III. Regression analyses are given in Table IV. Errors are quoted throughout as two standard deviations.

Banded gneisses. The data for the banded gneiss samples are plotted in the $^{87}Sr/^{86}Sr$ versus $^{87}Rb/$

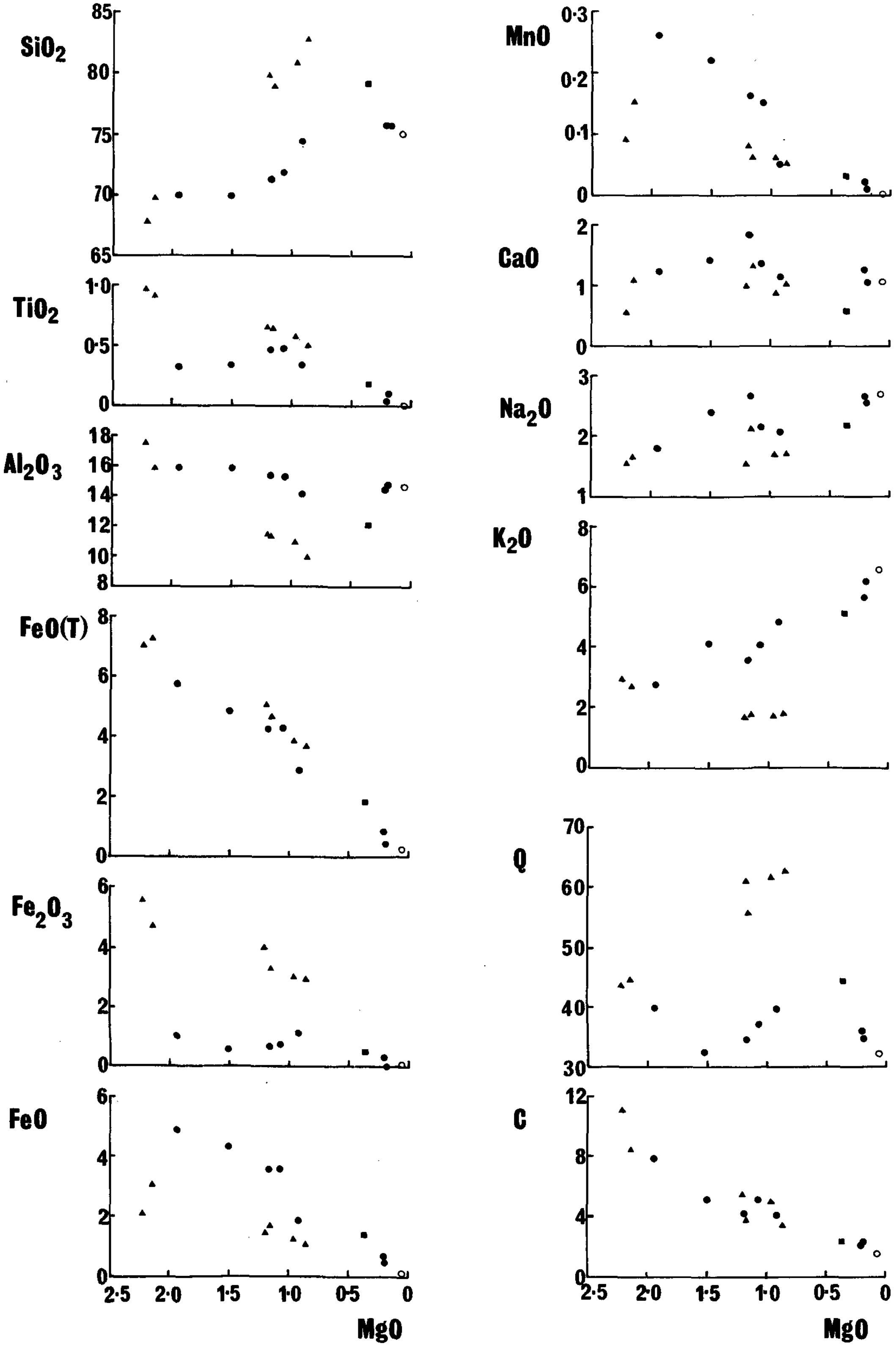

FIG. 2. Variation diagrams of oxides and normative Q and C. All figures in per cent. Filled circles: migmatites MB 53, 60–65. Open circle: migmatite leucosome MB 61L. Triangles: banded gneisses MB 52, 55–59. Square: MB 54.

TABLE III. *Rb–Sr results*

Rock type	Sample No.	Rb ppm	Sr ppm	^{87}Rb/^{86}Sr	Two standard deviations	^{87}Sr/^{86}Sr	Two standard deviations
Banded gneiss whole rock	MB 52	34.5	141	0.709	±0.007	0.72956	±0.00025
	MB 54	164	45.1	10.95	±0.11	1.07092	±0.00082
	MB 55	39.5	132.1	0.868	±0.009	0.73460	±0.00025
	MB 56	56.7	145	1.136	±0.011	0.74574	±0.00025
	MB 57	33.7	132	0.741	±0.007	0.73287	±0.00025
	MB 58	26.9	118	0.660	±0.007	0.72779	±0.00025
	MB 59	72.3	146	1.438	±0.014	0.75440	±0.00036
Migmatite whole rock	MB 53	233	150	4.56	±0.05	0.85317	±0.00025
	MB 60	94.9	129	2.149	±0.021	0.81698	±0.00025
	MB 61	195	145	3.95	±0.04	0.82931	±0.00025
	MB 61L	232	152	4.47	±0.04	0.83685	±0.00025
	MB 62	134	123	3.20	±0.03	0.83267	±0.00025
	MB 63	95.1	90.4	3.07	±0.03	0.82545	±0.00025
	MB 64	162	124	3.84	±0.04	0.86218	±0.00025
	MB 65	173	127	3.99	±0.04	0.84007	±0.00025
MB 60 Minerals	Plag	8.10	133	0.177	±0.014	0.79078	±0.00025
	Kfel	99.7	146	1.99	±0.04	0.81629	±0.00025
	Bio	651	13.3	170.5	±2.5	2.932	±0.038

The Rb and Sr concentrations are accurate to about ±5% (two standard deviations).
Whole rock Rb/Sr ratios were determined by XRF in replicate.
^{87}Sr/^{86}Sr ratios were determined in duplicate (the MB 60 biotite in quadruplicate).
Errors given are based on pooled errors on replicate analyses (*c*.50 degrees of freedom) except for: (*a*) mineral Rb/Sr ratios which were determined by isotope dilution, the errors being calculated for each determination; (*b*) the error in the biotite ^{87}Sr/^{86}Sr ratio, which was based on the reproducibility of the four analyses; (*c*) the error in the ^{87}Sr/^{86}Sr ratio for MB 54 which is based on replication of that value alone because of the poor reproducibility.

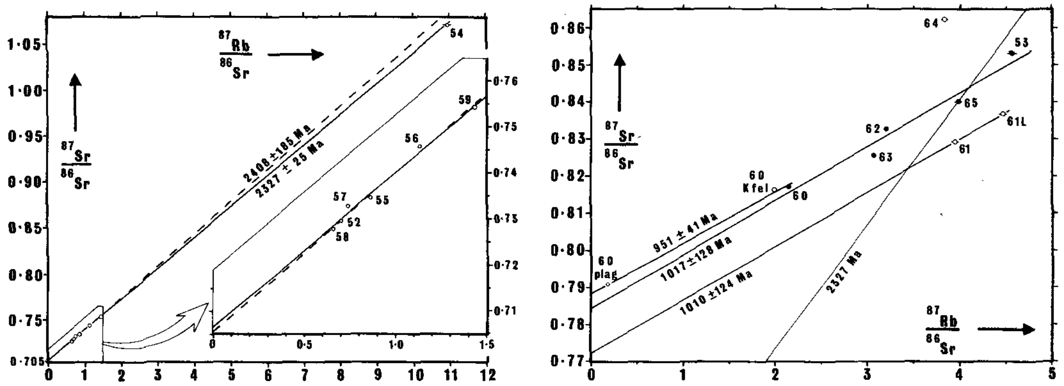

FIGS. 3 and 4. FIG. 3 (*left*). Plot of ^{87}Sr/^{86}Sr versus ^{87}Rb/^{86}Sr for data from the banded gneisses (Table III). The dashed line is the (extrapolated) regression line for all but MB 54. The solid line is the regression line for all seven data points (see Table IV). FIG. 4 (*right*). Plot of ^{87}Sr/^{86}Sr versus ^{87}Rb/^{86}Sr for data from the migmatites (Table III). The sub-parallel lines are all regression lines giving estimates of the date *c*.1000 Ma event (see text). The steeper line is the banded gneiss isochron superimposed for comparison. The data points marked by solid symbols were those used to obtain the 1017 Ma regression line (see Table IV).

TABLE IV. *Results of regression analyses*

Rock type	Samples used	Age ± 2s Ma	Intercept ± 2s	F_c	5% F
Banded gneiss	All but MB 54	2408 ± 52 2408 ± 185	0.7054 ± 0.0006 0.7054 ± 0.0023	32.59 2.61	2.61
	All	2327 ± 24 2327 ± 25	0.7064 ± 0.0003 0.7064 ± 0.0003	2.73 2.45	2.45
Migmatite whole rocks	MB 53, 60, 62, 63, 65	1017 ± 20 1017 ± 128	0.7844 ± 0.0009 0.7844 ± 0.0058	113.1 2.84	2.84
	53, 60, 61, 61L, 62, 63, 64, 65	1414 ± 26 1414 ± 533	0.7655 ± 0.0013 0.765 ± 0.025	949.7 2.34	2.34
	61, 61L	1010 ± 124	0.772 ± 0.007	—	—
Migmatite minerals (MB 60)	Plag, Kfel	982 ± 28	0.7883 ± 0.0005	—	—
	Plag, Kfel whole rock*	951 ± 22 951 ± 41	0.7884 ± 0.0005 0.7884 ± 0.0010	14.88 4.08	4.08
	Plag, Kfel, whole rock, bio	916 ± 14	0.7891 ± 0.0004	0.01	3.23
	Bio, **(O, 0.7064 ± 3)	913 ± 20	0.7064 ± 0.0003	—	—

* MB 60 whole-rock data as in Table III except that the error in ^{87}Rb/^{86}Sr was increased from ± 1.00 % (0.021) to ± 1.41 % (0.030) to take account of the statistical error in calibration between XRF and isotope dilution.

** Initial ^{87}Sr/^{86}Sr ratio of the banded gneisses.

All ages were calculated using a ^{87}Rb decay constant of $1.42 \times 10^{-11} a^{-1}$.

F_c is the calculated variance ratio.

5 % F is the limiting value of F at the 5 % level.

2s means two standard deviations.

All regression lines were calculated according to the method of Williamson (1968).

^{86}Sr diagram fig. 3. They yield a regression line giving an apparent age of 2327 ± 24 Ma (2.73: ± 25 Ma) and an initial ^{87}Sr/^{86}Sr ratio of 0.7064 ± 0.0003 (0.0003). Regressing all but MB 54, which dominates the apparent age (fig. 3 and Table IV), the banded gneisses yield a regression line that exhibits excess scatter but the age of 2408 ± 52 Ma (32.6: ± 185 Ma) is indistinguishable from the seven-point regression line within the expanded errors. Thus the best regression line is that given by all seven points.

Migmatites. The whole-rock data for the migmatite samples are plotted in fig. 4. It can be seen that the data points do not define an isochron. There is a strong correlation, however, between five of the samples (excluding MB 61, 61L, and 64). These form a regression line giving an apparent age of 1017 ± 20 Ma (113.1: ± 128 Ma) and intercept of 0.7844 ± 0.0009 (± 0.0058).

In order to test the meaning of this correlation, data (Table III, fig. 4) for the 400 g sample of leucosome, MB 61L, were combined with those for its parent MB 61; these two points give a model age of 1010 ± 124 Ma and an intercept of 0.772 ± 0.007. In addition, plagioclase, alkali feldspar, and biotite were separated from whole-rock sample MB 60. They were analysed by isotope dilution using ^{84}Sr-enriched and ^{87}Rb-enriched spikes. Independent measurements were made of the ^{87}Sr/^{86}Sr ratios on unspiked aliquots of stock sample solutions. The biotite showed poor reproducibility of ^{87}Sr/^{86}Sr ratios on replicate solutions. The mean of four analyses was taken (Table III). Both concentration and isotopic abundance measurements for Sr were corrected for blank although this is not critical in this case. The feldspars together with the whole rock yield a regression line giving 951 ± 22 Ma (14.9: ± 41 Ma) for the apparent age and 0.7884 ±

0.0005 (±0.0010) for the intercept. Regressing these data together with the biotite analysis yields a line giving an apparent age of 916±14 Ma (0.01) and a $^{87}Sr/^{86}Sr$ initial ratio of 0.7891±0.0004.

The migmatite samples were thus clearly affected by a heating event about 1000 Ma ago, which caused only partial resetting of the strontium isotopes and which was preceded by a long period in the earth's crust (shown by the high initial $^{87}Sr/^{86}Sr$ ratio of about 0.78). Because of the geographical proximity of the banded gneisses and migmatites, there is little doubt that the migmatites were affected by the 2327 Ma event as well as by the 1000 Ma event. The way in which the migmatite data plot about the banded gneiss regression line (fig. 4) is consistent with this conclusion.

As there are three independent estimates of the age of the 1000 Ma event, but of differing quality, these estimates may be combined statistically (weighted according to the expanded errors) to yield a best estimate of the age, even though each of the three estimates refer to different volumes of the rock, which we here term 'domains'. The three domains are: (1) the MB 60 feldspars plus whole rock, giving 951±41 Ma; (2) the small domain of MB 61 and MB 61L, giving 1010±124 Ma; (3) the large domain of MB 53, 60, 62, 63, and 65, giving 1017±128 Ma. Combined they give a best estimate of 962±34 Ma for the age of the 1000 Ma event.

The three minerals and the whole-rock point from MB 60 yield an isochron which is dominated by the biotite data point. Thus the age of 916±14 Ma is interpreted as the date that the biotite became a closed system to diffusion of radiogenic ^{87}Sr as the crust underwent uplift and cooling. According to Purdy and Jaeger (1976) this would have occurred at a temperature of 300 °C. On the theory that under open system behaviour all the radiogenic ^{87}Sr will diffuse out of the biotite leaving only that Sr that was accommodated in the crystal lattice at its formation, one can calculate a model biotite age using the banded gneiss isochron initial $^{87}Sr/^{86}Sr$ ratio. This model age is 913±20 Ma (Table IV). The two ages are limiting cases and are indistinguishable. The first (based on more data) is taken as the best estimate of the biotite cooling age. It is indistinguishable from 962±34, which is the best estimate of the date of culmination of the *c.*1000 Ma heating event.

The homogenization of $^{87}Sr/^{86}Sr$ approached completion during the 1000 Ma event only over domains of limited size. Within each domain, the $^{87}Sr/^{86}Sr$ value in any individual volume of rock tended towards the mean value of that variable for the domain. This process of partial homogenization on a domain basis provides an explanation for the fact that some samples (notably MB 64) experienced very considerable resetting of the strontium isotopes, departing substantially from the 2327 Ma regression line, but the movement was not towards any regression line which could reasonably be postulated to represent the migmatite area as a whole.

Regional setting

In his description of the geology of the area, Peters (1975) found that the structures and metamorphism in the Champira Dome could not be related to those of the surrounding area. The dome also differs from its surroundings in the presence of abundant dolerite dykes (Peters, 1975) and in the existence of a strong positive gravity anomaly (about 25 mgal) (Andrew, 1974) which may be caused by a large body of basic rock (possibly the feeder for the dolerite dykes) underlying the exposed rocks at shallow depth.

Although no dates are available for the pre-600 Ma metamorphic history of the area surrounding the Champira Dome, the ages of the principal orogenic events are remarkably constant over Africa as a whole, the earliest orogenies (before 2500 Ma) being followed by others at 1850±250 Ma, 1100±200 Ma, and 600 Ma ago. In the present study, the *c.*1000 Ma partial resetting of the Sr isotopes in the migmatite samples can be correlated with the Kibaran (Irumide) orogeny (although elsewhere in Malawi and Zambia this orogeny is characterized by plutonism and low-grade metamorphism), but there is no known analogue for the *c.*2300 Ma date obtained for the banded gneisses (see, for example, Snelling *et al.*, 1972; Carter and Bennett, 1973; Clifford, 1974).

Discussion

Various interpretations may be advanced for the mineralogical and geochemical features described in this paper.

The first is that the present mineralogy was formed during a single metamorphism *c.*1000 Ma ago and that the strontium isotope homogenization at *c.*2300 Ma represents diagenesis or a pre-1000 Ma metamorphism of which all petrographic evidence has since been erased. If the rocks were affected by the 1850±250 Ma (Ubendian) event, no mineralogical features remain. The only replacement textures seen in the banded gneisses (the formation of cordierite at the expense of sillimanite and probably also of biotite) are consistent with crystallization during a single phase of metamorphism. The development of a garnet–biotite–sillimanite assemblage in the migmatites and the subsequent growth of cordierite from these minerals requires (see data of Holdaway and Lee,

1977) (1) a decrease in P_{tot}, (2) an increase in P_{H_2O} at constant P_{tot}, matched by an appropriate increase in T (too high or too low an increase in T would result in a different assemblage), or (3) a decrease in the ferrous-iron content (by oxidation). The first of these necessitates a substantial time interval for erosion, but the other two could be accomplished by the necessary changes of conditions within a single phase of metamorphism. During the 1000 Ma metamorphism, on this hypothesis, the strontium isotopes in the banded gneisses were almost undisturbed on the scale of sampling, but the melting of pelitic rocks to produce the migmatites resulted in major disturbance, though not large-scale homogenization.

In favour of this hypothesis is that the 2327 ± 25 Ma regression line can be accepted as representing strontium isotope homogenization without requiring a metamorphism at a date at which there is no known metamorphism in the region. Against this, however, may be set the improbability that the strontium isotopes could be so thoroughly homogenized during diagenesis and yet so little mobilized during high-grade metamorphism and anatexis. The behaviour of strontium isotopes during metamorphic processes is still imperfectly understood, but there is sufficient published evidence of their mobility to make this hypothesis unlikely.

Most Rb-Sr studies of metasediments have dealt with pelitic rocks (an exception is the work of Spanglet *et al.* (1978) showing that in both diagenesis and metamorphism psammitic rocks suffer less strontium isotope disturbance than pelites), and the sample localities have generally been closer together than in the present study. Rb-Sr whole-rock isochrons in shales, slates, and phyllites have been variously attributed to deposition, diagenesis, and low-grade metamorphism (e.g. Bofinger and Compston, 1967; Moorbath, 1969; Bofinger *et al.*, 1970; Pankhurst, 1974) but these rocks have not undergone subsequent high-grade metamorphism. Doig (1977) concluded that the first high-grade metamorphism of pelitic sediments normally homogenized the strontium isotopes on outcrop scale, and other workers have recorded metamorphic resetting over distances of several km (e.g. Pidgeon and Råheim, 1972; Moorbath and Taylor, 1974; Clifford *et al.*, 1975). Brewer *et al.* (in press) have shown that prograde metamorphism of pelites in the lower amphibolite facies (*c.*1000 Ma old) to mid/upper amphibolite facies *c.*400 Ma ago resulted in thorough recrystallization and resetting of Sr isotope ratios within domains on a scale of *c.*10^6 m^3.

The presence of a fluid phase is clearly critical to the large-scale homogenization of strontium isotope ratios, and the mobility of this fluid will determine the extent of homogenization. Margaritz and Hofmann (1978) showed that diffusion rates of strontium ions are very low, and there is ample evidence that strontium isotope ratios may survive metamorphism relatively undisturbed in granitic rocks in the absence of a fluid exchange medium (e.g. Brook *et al.*, 1976; Gray and Compston, 1978). Krogh and Davis (1973) showed that Rb-Sr systematics in granitic rocks were quite unaffected by metamorphism while the border zone between granite and amphibolite, where the growth of biotite proved the presence of a mobile fluid phase, gave a Rb-Sr whole-rock isochron age for the (amphibolite facies) metamorphism. In contrast, open-system behaviour in acid igneous rocks can give rise to a Rb-Sr whole-rock isochron which reflects no known geological event (Page, 1976; Brewer *et al.*, 1979*b*).

Whatever the mineral content of the parent sediments of the banded gneisses immediately before metamorphism, it is improbable that they contained neither hydrous minerals nor pore fluid. It would therefore be expected that, on the outcrop scale at least, the strontium isotopes would have been mobilized during the thorough recrystallization brought about by the first (or only) high-grade metamorphism, and it is improbable that a diagenetic whole-rock isochron would be retained without major disturbance. If the gneisses were subjected to a second metamorphism with no change to their mineralogy, the Rb-Sr systematics would be expected to be largely unaffected.

The processes of granitization involve resetting of strontium isotopes, at very least at outcrop scale and probably on a much larger scale (e.g. Hofmann and Köhler, 1973; Brook *et al.*, 1976; Stueber and Heimlich, 1977). The anatexis in the Champira Dome could therefore be expected to equilibrate at least the closer migmatite samples such as MB 62 and 63 (less than 50 m apart).

The second hypothesis is that there was a single metamorphism, 2327 ± 25 Ma ago, and that the *c.*1000 Ma episode had no metamorphic effects. This offers a credible interpretation of the 2327 ± 25 Ma regression line, but it does not account for the contrast between the considerable disturbance of the strontium isotopes at *c.*1000 Ma in the migmatites (which are here supposed to be dry rocks which experienced no recrystallization) and the relative stability of the banded gneisses.

Another difficulty about this interpretation is that there is no other published evidence for a metamorphism *c.*2300 Ma ago in the region: the Champira Dome would fit more readily into the metamorphic history of the continent if an older age (> 2500 Ma) for the metamorphism could be postulated. The dome could then be seen as part of one of the ancient nuclei of Africa. Regression of MB 62, 63, and 64 with MB 52 and 55–59, for example, gives an age of 2817 ± 20 Ma and an initial ratio of 0.7005 ± 0.0003, with F_c 19.7 and 5 % F 2.25. On this basis, most of the samples, including MB 54, lost radiogenic strontium during subsequent metamorphisms (*c.*1000 Ma and possibly also *c.*1800 Ma), and MB 60 gained radiogenic strontium. The MB 61–MB 61L and MB 60 mineral regression lines may be taken to show that small-scale homogenization took place *c.*1000 Ma ago. This hypothesis can offer a reasonable age for the granulite-facies metamorphism, but only by ignoring the good banded gneiss regression line of 2327 ± 25 Ma.

The third interpretation of the data is that the two phases of metamorphic crystallization recorded in the migmatites may be correlated with the two episodes of strontium isotope mobility *c.*2300 Ma and *c.*1000 Ma ago. The early metamorphism raised the banded gneisses to their present mineral assemblages and brought about anatexis in what are now the migmatites. During the second metamorphism the banded gneisses were essentially undisturbed but in the migmatites cordierite grew at the expense of garnet, sillimanite, and biotite with the consequent release of water and recrystallization of the felsic minerals. The radiogenic strontium was thus mobilized more in the migmatites than in the banded gneisses, though the disturbance was insufficient to reset the Rb–Sr system on the scale of sampling. The samples which plot furthest from the 1017 ± 128 Ma migmatite regression line are MB 61 and MB 64, in which cordierite is rare or absent.

Although the problem of the date of the earlier metamorphism remains (and probably cannot be solved on present evidence), this interpretation is preferred to the second because it offers a geological explanation for the contrast in strontium isotope mobility at *c.*1000 Ma between the two suites. It is preferred over the first interpretation because it is more consistent with present knowledge about the behaviour of strontium isotopes during metamorphism. On present evidence the authors favour the acceptance of the 2327 ± 25 Ma regression line as giving the date of high-grade metamorphism and anatexis and the 962 ± 34 Ma age as the date of a subsequent biotite–cordierite–almandine-subfacies metamorphic recrystallization in the migmatite samples.

Summary and conclusions

(1) Two suites of siliceous and aluminous rocks are described. One suite, the migmatites, was formed by anatexis from a succession of potash-rich sandy clays. The other suite, the banded gneisses, was metamorphosed with only minor, local anatexis confined to rocks with low normative An contents. These gneisses were derived from more arenaceous sediments, which contained alkali feldspar and abundant quartz and were distinguished chemically from the parent sediments of the migmatites by higher oxidation ratios and higher Ba/Rb ratios.

Garnet, sillimanite, and biotite crystallized as the principal silicate refractory minerals in the migmatites. These minerals were subsequently partly replaced by cordierite, with the recrystallization of the felsic minerals. The cordierite–garnet–biotite–sillimanite paragenesis suggests conditions of, very approximately, 675 °C, 5 kb, and $P_{H_2O} = 0.4\ P_{tot}$.

(2) The anatexis which led to the formation of the migmatites followed the path described by Winkler (1976) in the water-saturated system Q–Or–Ab–An. Analytical data from a rock that apparently represents a liquid formed during this melting plot almost on the quartz + alkali feldspar + melt + gas cotectic surface. This melt, and the migmatites with the lowest content of refractory minerals, have a high normative Or content which, though differing markedly from the compositions of most granitic rocks and of eutectic melts in the water-saturated system Q–Or–Ab, has been shown by Winkler to be characteristic of anatectic liquids formed in the water-saturated system Q–Or–Ab–An.

The widespread melting did not lead to the production of magmas with normal igneous chemical and mineralogical composition. Instead of a typical igneous texture comprising early and late formed magmatic minerals, the migmatites retain a texture of leucosome plus restite. This is a reflection both of incomplete melting and of the chemical composition of the parent pelites: the low CaO content prevented the formation of hornblende and the high Al_2O_3 led to the growth and survival of the aluminous phases sillimanite, garnet, cordierite, and hercynite.

The composition of the leucosome MB 61L suggests conditions of anatexis of 670–685 °C at 7–5 kb if $P_{H_2O} = P_{tot}$, but if P_{H_2O} was less than P_{tot}, higher temperature and pressure would have been required. The oxide phases appear to have formed by unmixing of a primary magnetite–hercynite solid solution which requires a higher temperature to form, so it may be that the temperature locally attained 700–800 °C.

(3) The relative stabilities of garnet and cordierite are sensitive to the molar FeO/(FeO + MgO) ratio of the rock: where this ratio is below 0.45 cordierite occurs alone; where it is 0.53–0.64 cordierite co-

exists with relic garnet; and where it is above 0.64 garnet occurs without cordierite.

(4) The compositions of the oxide minerals indicate equilibration during post-metamorphic cooling. The association magnetite-hercynite-corundum in the migmatites is thought to have formed by unmixing of a homogeneous Fe_3O_4-$FeAl_2O_4$ solid solution, illustrating the phase relationships established by experimental work (Turnock and Eugster, 1962). Hematite-ilmenite-corundum associations in the banded gneisses are, similarly, thought to result from the unmixing of a high temperature Fe_2O_3-$FeTiO_3$-Al_2O_3 solid solution.

(5) The banded gneisses yield a Rb-Sr whole-rock age of 2327 ± 25 Ma, with an initial $^{87}Sr/^{86}Sr$ ratio of 0.7064 ± 0.0003, which indicates a short prior crustal history. The migmatite data relate to this regression line in such a way as to be consistent with homogenization of strontium isotopes at the same time, but as a result of subsequent disturbance they no longer define an isochron of that age.

During this later event there was no disturbance of the whole-rock strontium isotope systems in the banded gneisses. In the migmatites, partial homogenization of the strontium isotopes throughout the volume sampled was accompanied by partial homogenization within small local domains. Thus each sample tended to equilibrate towards the mean $^{87}Sr/^{86}Sr$ ratio for its immediate environment and at the same time also showed a tendency to move towards the mean for the whole migmatite body. The samples in which there was breakdown of biotite, with consequent release of water and recrystallization of the felsic minerals, show the nearest approach to equilibration over the whole area and, with one other sample, yield a five-point regression line with an age of 1017 ± 128 Ma. Two samples in which there was little or no breakdown of biotite lie off this regression line, having equilibrated only towards the mean of their local domains. The best estimate for the age of this event is 962 ± 34 Ma.

(6) Of the various interpretations that may be placed on the data, it is thought most likely that the 2327 ± 25 Ma date represents the metamorphism of the banded gneisses and the anatexis in the migmatites. The 962 ± 34 Ma date in the migmatites is thought to date a later metamorphism in which cordierite formed at the expense of garnet, sillimanite, and biotite, while the mineral assemblages of the banded gneisses remained stable.

Acknowledgements. We wish to express our thanks to the staff of the Geological Survey of Malawi for assistance in the collection, crushing and splitting of the samples, to J. F. W. Bowles for instruction and assistance in the use of the electron probe, and to N. J. Snelling and R. J. Pankhurst for criticism of the manuscript. The work is part of an overseas aid project funded by the Ministry of Overseas Development through the Overseas Division of the Institute of Geological Sciences, the staff of which we wish to thank for their interest and support. The paper is published by permission of the Director of IGS and the Chief Geologist, Geological Survey of Malawi.

REFERENCES

Andrew (E. M.), 1974. *Rep. Inst. Geol. Sci.* **74**/15.

Ashworth (J. R.) and Chinner (G. A.), 1978. *Contrib. Mineral. Petrol.* **65**, 379–94.

Bofinger (V. M.) and Compston (W.), 1967. *Geochim. Cosmochim. Acta*, **31**, 2353–9.

—— —— and Gulson (B. L.), 1970. Ibid. **34**, 433–45.

Bowles (J. F. W.), 1975. *Rep. Inst. Geol. Sci.* **75**/9.

Brewer (M. S.), Brook (M.), and Powell (D.), in press. In *The Caledonides of the British Isles—reviewed 1979*. Geol. Soc. Lond.

—— Haslam (H. W.), Darbyshire (D. P. F.), and Davis (A. E.), 1979*a*. *Rep. Inst. Geol. Sci.* **79**/1.

—— —— —— —— 1979*b*. Ibid. **79**/5.

Brook (M.), Brewer (M. S.), and Powell (D.), 1976. *Nature*, **260**, 515–17.

Buddington (A. F.) and Lindsley (D. H.), 1964. *J. Petrol.* **5**, 310–57.

Carter (G. S.) and Bennett (J. D.), 1973. *Bull. Geol. Surv. Malawi*, **6** (2nd revised edition).

Clifford (T. N.), 1974. *Spec. Pap. Geol. Soc. Am.* 156.

—— Gronow (J.), Rex (D. C.), and Burger (A. J.), 1975. *J. Petrol.* **16**, 54–88.

de Waard (D.), 1965. *Am. J. Sci.* **263**, 455–61.

Doig (R.), 1977. *Geol. Soc. Am. Bull.* **88**, 1843–56.

French (W. J.) and Adams (S. J.), 1972. *Analyst*, **97**, 828–31.

Gray (C. M.) and Compston (W.), 1978. *Geochim. Cosmochim. Acta*, **42**, 1735–47.

Heier (K. S.) and Billings (G. K.), 1970. In *Handbook of geochemistry*, Wedepohl (K. H.) (ed.), Berlin-Heidelberg-New York (Springer), **II/2**, 37D 1–4, 37G1–2, 37K1–3.

Hofmann (A.) and Köhler (H.), 1973. *N. Jb. Miner. Abh.* 119, 2, 163–87.

Holdaway (M. J.), 1971. *Am. J. Sci.* **271**, 97–131.

—— and Lee (S. M.), 1977. *Contrib. Mineral. Petrol.* **63**, 175–98.

Hsu (H. L.), 1968. *J. Petrol.* **9**, 40–83.

Kleeman (A. W.), 1965. *J. Geol. Soc. Aust.* **12**, 35–52.

Krogh (T. E.) and Davis (G. L.), 1973. *Carnegie Inst. Washington Year Book*, **72**, 601–10.

Le Maitre (R. W.), 1976. *J. Petrol.* **17**, 589–637.

Margaritz (M.) and Hofmann (A. W.), 1978. *Geochim. Cosmochim. Acta*, **42**, 595–605.

Mason (P. K.), Frost (M. T.), and Reed (S. J. B.), 1969. N.P.L. (I.M.S.), Report No. 2.

Moorbath (S.), 1969. *Scott. J. Geol.* **5**, 154–70.

—— and Taylor (P. N.), 1974. *Nature*, **250**, 41–3.

Page (R. W.), 1976. *Carnegie Inst. Washington Year Book*, **75**, 813–21.

Pankhurst (R. J.), 1974. *Geol. Soc. Am. Bull.* **85**, 345–50.

Peters (E. R.), 1975. *Bull. Geol. Surv. Malawi*, **36**.

Pidgeon (R. T.) and Råheim (A.), 1972. *Norsk Geol. Tidsskrift*, **52**, 241-56.

Puchelt (H.), 1972. In *Handbook of geochemistry*, Wedepohl (K. H.) (ed.), Berlin-Heidelberg-New York (Springer), **II/3**, 56D1-18, 56G1, 56K1-8.

Purdy (J. W.) and Jaeger (E.), 1976. *Mem. 1st Geol. Min. Univ. Padova*, 30.

Richardson (S. W.), Gilbert (M. C.), and Bell (P. M.), 1969. *Am. J. Sci.* **267**, 259-72.

Roberts (J. L.) and Davis (A. E.), 1977. *Rep. Inst. Geol. Sci.* **77**/3.

Snelling (N. J.), Johnson (R. L.), and Drysdall (A. R.), 1972. *Rec. Geol. Surv. Zambia*, **12**, 19-30.

Spanglet (M.), Brueckner (H. K.), and Senechal (R. G.), 1978. *Geol. Soc. Am. Bull.* **89**, 783-90.

Stormer (J. C.), 1975. *Am. Mineral.* **60**, 667-74.

Stueber (A. M.) and Heimlich (R. A.), 1977. *Geol. Soc. Am. Bull.* **88**, 441-4.

Tait (B. A. R.) and Coats (J. S.), 1976. *Rep. Inst. Geol. Sci.* **76**/11.

Turnock (A. C.) and Eugster (H. P.), 1962. *J. Petrol.* **3**, 533-65.

Tuttle (O. F.) and Bowen (N. L.), 1958. *Geol. Soc. Am. Mem.* **74**.

Williamson (J. H.), 1968. *Can. J. Phys.* **46**, 1845-7.

Winkler (H. G. F.), 1976. *Petrogenesis of metamorphic rocks* (4th edition). New York-Heidelberg-Berlin (Springer-Verlag).

[*Manuscript received 19 July 1979;*
revised 8 January 1980]